Atmospheric Environment 355 (2025) 121257

Contents lists available at ScienceDirect

Atmospheric Environment

journal homepage: www.elsevier.com/locate/atmosenv

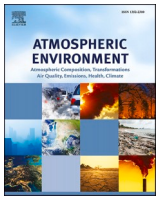

Comparison of traffic-related micro- and nanoplastic concentrations at three urban locations

E.S. Lenssen [a,*], L. Scibetta [b], M. Brits [b,c], M. Lamoree [b], L. Caiazzo [d], M.R. Montereali [d], S. Manzo [e], S. Chiavarini [d], R. Vermeulen [a], R.H.H. Pieters [a], G. Hoek [a]

[a] Institute for Risk Assessment Sciences, Utrecht University, Utrecht, the Netherlands
[b] Amsterdam Institute for Life and Environment, Vrije Universiteit, Amsterdam, the Netherlands
[c] The Southern African Grain Laboratory (SAGL), Grain Building-Agri Hub Office Park, 477 Witherite Street, The Willows, Pretoria, 0040, South Africa
[d] ENEA, C.R. Casaccia, Rome, Italy
[e] ENEA C.R. Portici, Naples, Italy

HIGHLIGHTS

- Compared to urban park, tyre-wear levels were 2–5 fold higher near major roads.
- Similar contrasts were observed for black carbon and brake-wear related components.
- Tyre-wear levels were modestly higher than the analytical noise of field blanks.
- Moderate to high correlations were observed between tyre- and brake-wear pollutants.

ARTICLE INFO

Keywords:
Microplastics
Pyrolysis-gas chromatography-mass spectrometry
Rubber
Tyre- and road wear particles
Traffic-related air pollution
Motorized road traffic
Atmospheric exposure

ABSTRACT

One predominant source of microplastics emitted into the atmosphere is tyre- and road wear particles (TRWPs). Only a handful of studies have quantified atmospheric TRWP concentrations. Our objective was to study variations in TRWPs, compared to other primary traffic pollutants, at locations with different traffic conditions.

In 2022–2023, three locations with different traffic-flow and speed (a stop-and-go busy road, highway and urban park), were repeatedly visited for 4-hrs resulting in 23 measurement days. Particles were collected on quartz filters using a high-volume sampler with PM_{10}-inlet and analyzed using double-shot pyrolysis-gas chromatography-mass spectrometry for the mass of synthetic- and natural rubbers (NR). Concentrations of combustion and brake-wear-related traffic air pollutants were measured, including PM_{10}, black carbon (BC), ultrafine particles (UFP) and trace elements. We calculated spatial contrasts and correlations.

We observed relatively low levels of sampling- and analysis rubber marker contamination. Synthetic- and NR levels ranged between 2.9 to 42.5 ng/m^3 and 1.6 to 26.8 ng/m^3, respectively. Compared to the park, rubber markers were 2.8 to 4.6 times higher at the stop-and-go and 2.0 to 2.7 times higher at the highway. These contrasts were larger than for UFP and PM_{10}, but similar to BC and brake-wear related components. Park synthetic rubber levels were modestly higher than field blanks. Rubber markers were highly correlated ($r = 0.66$ to 0.98) and weakly correlated with most other air pollutants, except for BC and brake wear-related trace elements ($r = 0.36$ to 0.77).

We found substantially increased atmospheric TRWP levels near major roads compared to a park. The measurements from this study will be used for testing associations with health effects.

* Corresponding author. Yalelaan 2, 3584 CM, Utrecht, the Netherlands.
E-mail addresses: e.s.lenssen@uu.nl (E.S. Lenssen), l.scibetta@vu.nl (L. Scibetta), m.brits@vu.nl (M. Brits), marja.lamoree@vu.nl (M. Lamoree), laura.caiazzo@enea.it (L. Caiazzo), mariarita.montereali@enea.it (M.R. Montereali), sonia.manzo@enea.it (S. Manzo), salvatore.chiavarini@enea.it (S. Chiavarini), r.vermeulen@uu.nl (R. Vermeulen), r.h.h.pieters@uu.nl (R.H.H. Pieters), g.hoek@uu.nl (G. Hoek).

https://doi.org/10.1016/j.atmosenv.2025.121257
Received 4 December 2024; Received in revised form 9 April 2025; Accepted 21 April 2025
Available online 24 April 2025

1. Introduction

Micro- and nanoplastics (MNPs) is a collective term for a heterogeneous group of plastic degradation products polluting the environment. MNPs result from intentional manufacturing (primary) or various fragmentation processes (secondary) induced by weathering, high temperatures, biological breakdown and/or UV-radiation. MNPs have been reported in both natural and anthropogenic environments and their presence is attributed to various sources, including synthetic clothes/textiles, building materials, plastic products, waste and landfilling (Dris et al., 2015; Maurizi et al., 2024; Nafea et al., 2024). MNPs generated by abrasion of tyres from motorized vehicles are often suggested to be one of the main contributors of MNPs in the air (Browne et al., 2007; Jaikumar et al., 2019; Quik et al., 2024; Wang et al., 2020; Wright et al., 2017; Xu et al., 2024a). Uncertainty about quantitative emissions and concentrations is high (Panko et al., 2019; Park et al., 2018). In the Netherlands, it is estimated that each year approximately 880–2900 tons of plastic particles are released into the air due to tyre abrasion from road transport (Kole et al., 2017; Quik et al., 2024; Snijder and Nusselder, 2019; Verschoor, 2016). Due to the adoption of more stringent emission standards focused on decreasing pollutants derived from the combustion of fossil fuels and motor vehicles in particular, the relative contribution of the non-exhaust component to particulate matter with an aerodynamic size <10 μm (PM_{10}) levels has increased and is likely to increase further in the coming years (Denier van der Gon et al., 2013; Gouveia et al., 2006; Svensson et al., 2023). Electric vehicles reduce, at least locally, combustion-related pollutant emissions, but not the non-exhaust component (Jiang et al., 2022). As traffic is ubiquitous and roads are often positioned close to living spaces and cities, a relatively large number of people are (continuously) exposed to tyre wear particles. A better understanding of tyre wear particles and their potential health risks is therefore important.

Tyres comprise of a complex mixture of materials, including natural and synthetic rubber (e.g., styrene-butadiene and polybutadiene), which account for 5–70 % of their weight (Jeong et al., 2024). They also contain inorganic fillers (20–35 %, e.g., carbon black, silica), reinforcing materials (15 %), vulcanizing agents (2–5 %), accelerators and activators (0.5–1.5 %), as well as plasticizers and softeners (15–20 %) (Andersson-Sköld, 2020; Celeiro et al., 2021; van Broekhuizen, 2022; Vollertsen, 2018). The additives and vulcanizing agents are composed of numerous different chemicals. They may include adsorbed or absorbed compounds, such as trace metals, polycyclic aromatic hydrocarbons (PAHs), benzothiazoles and phthalates (Khan et al., 2024). The large uncertainty and heterogeneity in both emissions and concentrations can be attributed to a lack of experimental data, as concluded by Mennekes et al. (2022) and variations in sampling and analytical techniques. Moreover, the complexity of tyres, variations in tyre compositions due to the season or various manufacturers/brands and site- and time-specific factors (e.g., vehicle weight, tyre inflation, wheel alignment, type of pavement/road, weather conditions, driving habits) contribute to this heterogeneity (Mennekes et al., 2022).

Multiple studies have assessed different proxies for tyre wear, such as various trace elements (iron, copper, sulfur etc.), elemental carbon or soot (Almeida et al., 2020; Fomba et al., 2018). However, these markers are not unique to tyre wear, as they are also emitted from industrial- or traffic-combustion processes (such as soot or black carbon from diesel combustion), and motor oil (Lough et al., 2005; Dall'Osto et al., 2014). For iron (Fe) and copper (Cu) brake-wear is an important source (Schauer, 2006). Spectroscopic techniques, such as Fourier-Transform InfraRed Micro-spectroscopy (μFTIR) or scanning-electron microscopy (SEM) with a combination of either micro-Raman spectroscopy (μRaman) or elemental analysis using energy dispersive (EDX) detectors, have been used for more specific detection of single tyre and road wear particles (TRWPs) (Allegretta et al., 2022; Järlskog et al., 2022; Rausch et al., 2022). These spectroscopic techniques can provide detailed information on the number, morphology and size of the particles. Still, the high black carbon (BC) content can affect spectral quality and their current implementation is limited by low throughput.

Few studies have quantified the mass contribution of traffic-related MNPs in atmospheric samples using empirical data, with a focus on individual indicator compounds (e.g. styrene, dipentene, vinylcyclohexene) using thermal techniques (Blomqvist, 2023; Eisentraut et al., 2018; Liu et al., 2023; Müller et al., 2022; Panko et al., 2013, 2019). The main challenge for these methods is the uniqueness and stability of the marker(s) used for quantification (Khan et al., 2024). The most comprehensive studies have been performed by Panko et al. (2013; 2019) (Panko et al., 2013, 2019). They performed active measurements of PM2.5 and PM10 at various types of roadside locations throughout London, Tokyo and Los Angeles. Quartz filters were analyzed using Py-GC-MS focusing on indicator compounds styrene, 1,3-butadiene, vinyl-cyclohexene and dipentene. They observed an average TRWP level of 30 ng/m^3 for $PM_{2.5}$ and 160 to 960 ng/m^3 for PM_{10}, corresponding to a mass contribution of 0.23 % and 0.84 % to 1.94 % to total $PM_{2.5}$ and PM_{10}, respectively. In another study, Liu et al (2023) repeatedly collected atmospheric samples inside a tunnel for 3-hrs using a $PM_{2.5}$ inlet (Unice et al., 2012). Assessing Py-GC-MS markers dipentene and styrene, they observed a mean TRWP mass of 6522 ± 1455 ng/m^3, corresponding to a $PM_{2.5}$ mass contribution of about 4.7 %. Comparing absolute TRWP levels across studies is challenging due to substantial uncertainties in converting marker measurements into total TRWP mass, which complicates inter-study comparisons.

Given the knowledge gaps with regards to contrasts in exposure levels of traffic-related MNPs, this study aimed to quantify tyre-wear rubber exposure levels at urban locations varying in traffic intensity. The air sampling campaigns fit within the framework of a more extensive study to evaluate the health effects of short-term exposure to TRWPs, within a panel of healthy young adults. In the current paper we will give a detailed overview of the spatial and temporal variability of exposure levels of TRWPs, and compare this variability with other traffic-related pollutants in urban air. Other traffic-related air pollutants were additionally quantified, as traffic-related air pollutants exists of a complex mixture of exhaust and non-tailpipe emissions (Institute, 2022).

2. Methods

2.1. Study design

The current environmental exposure study is part of a semi-experimental study design, assessing health effects of short-term exposure to traffic-related MNPs in air. The study design was based on the RAPTES (Risk of Airborne Particles: A Toxicological-Epidemiological Hybrid Study) project (Strak et al., 2012). In total, 23 subjects were included in the panel study, who visited three different sites with varying traffic amounts and flow dynamics for 4-hrs. Sampling was generally conducted mid-day, between 11 and 15-hrs. These sites included a stop-and-go busy road, a highway and a park as urban background location. Each day samples were collected at one site. To limit potential temporal bias, we randomly rotated measurement days between the various measurement sites. During each 4-hr session, air samples were collected using a PM_{10} high-volume (HiVol) sampler and Harvard impactors, placed downwind from the potential local traffic source. Two synthetic and two natural rubber markers and benzothiazole were measured using Py-GC-MS. Non-exhaust particles typically follow a multimodal size distribution, with the largest peak around ~8 μm (Beji et al., 2020). TRWPs are predominantly generated within the larger PM_{10} fraction, contributing more significantly to the overall mass than smaller particle size-ranges such as $PM_{2.5}$ or ultrafine particles, as shown by a comprehensive previous study (Panko et al., 2019). Moreover, we focused on the PM_{10} fraction instead of total suspended particles due to its greater biological relevance. Additionally, other components of traffic-related air pollutants generated by either

combustion or brake-wear processes were measured, including concentrations of trace elements (e.g. iron, copper), PM_{10}, ultrafine particle number concentrations (PNC), BC, absorbance and PAHs.

2.1.1. Sampling sites

The sampling sites were chosen based on studies done by Strak et al (2011) and Piscitello et al. (2021) (Piscitello et al., 2021; Strak et al., 2011). For studying the health effects of traffic-related MNPs, we attempted to obtain contrast in MNPs not associated with the same contrast in other traffic-related air pollutants. We selected the sites based on the hypothesis that additional braking- and cornering from traffic would increase the contrast between MNPs released from tyres, relative to other traffic-related PM constituents from combustion such as PM_{10}, PNC and BC (Panko et al., 2019). Nonetheless, we realized that separating rubber tyre wear from brake wear (e.g. trace elements) by design is more challenging (Amato et al., 2020). Furthermore, the sampling sites had to meet the following requirements: 1) locations should have varying volumes of traffic and different flow dynamics, 2) to collect downwind measurements from the local source, it should be possible to position the measurement equipment on both sides of the road, 3) no noise barriers should be present, as these could reduce (large) particle concentrations and could interfere with accurate exposure measurements by altering wind patterns, 4) the distance between the sampling sites and the research facility should not exceed 30 min, to minimize potential exposure for the volunteers during transport, and 5) no other (industrial) sources of rubber emissions should be present around the sampling sites.

Sampling sites included a stop-and-go location nearby a round-about of an urban ring-road (Overvecht, Utrecht city), a highway with a high traffic intensity (Culemborg Diefdijk, outside city) and an urban background location (Wilhelminapark, Utrecht city) (Fig. 1 and Supplement Fig. S1). Utrecht is a city of about 360,000 inhabitants, located in the center of The Netherlands with extensive road infrastructure around the city. The stop-and-go location was a junction of the highway around Utrecht, ending in round-a-bout giving access to either the inner city or the ring of Utrecht. The highway was located 28 km outside Utrecht city center, which predominantly entailed continuous traffic. We did not encounter traffic jams during the sampling periods. The sampling equipment was placed on a viewing platform above the road, a setting comparable to the sites used by Strak et al (2011) (Strak et al., 2011). The urban background site was inside the largest park in the center of Utrecht. The nearest road was a minor road, located ~50 m from the site. The sampling inlets were placed ~1.5 m above the ground at all sites. The coordinates of the sampling sites can be found in Table S1.

2.2. Air sampling campaigns

Pilot air sampling campaigns were executed in 2021 and 2022, to optimize the sampling and downstream procedures for detection and quantification of traffic-related MNPs, including duration, flowrates, minimizing contamination and optimizing the sampling equipment required. As tyre MNPs are expected to contribute to only a small fraction of total PM_{10} mass in air, we needed large sampled volumes to reach analytical detection limits. Our main sampling instrument was therefore a Hivol sampler with a PM_{10} inlet. The duration of the sampling, 4-hrs, was based on the semi-experimental study as a compromise between the exposure being sufficiently different from normal traffic exposures and a

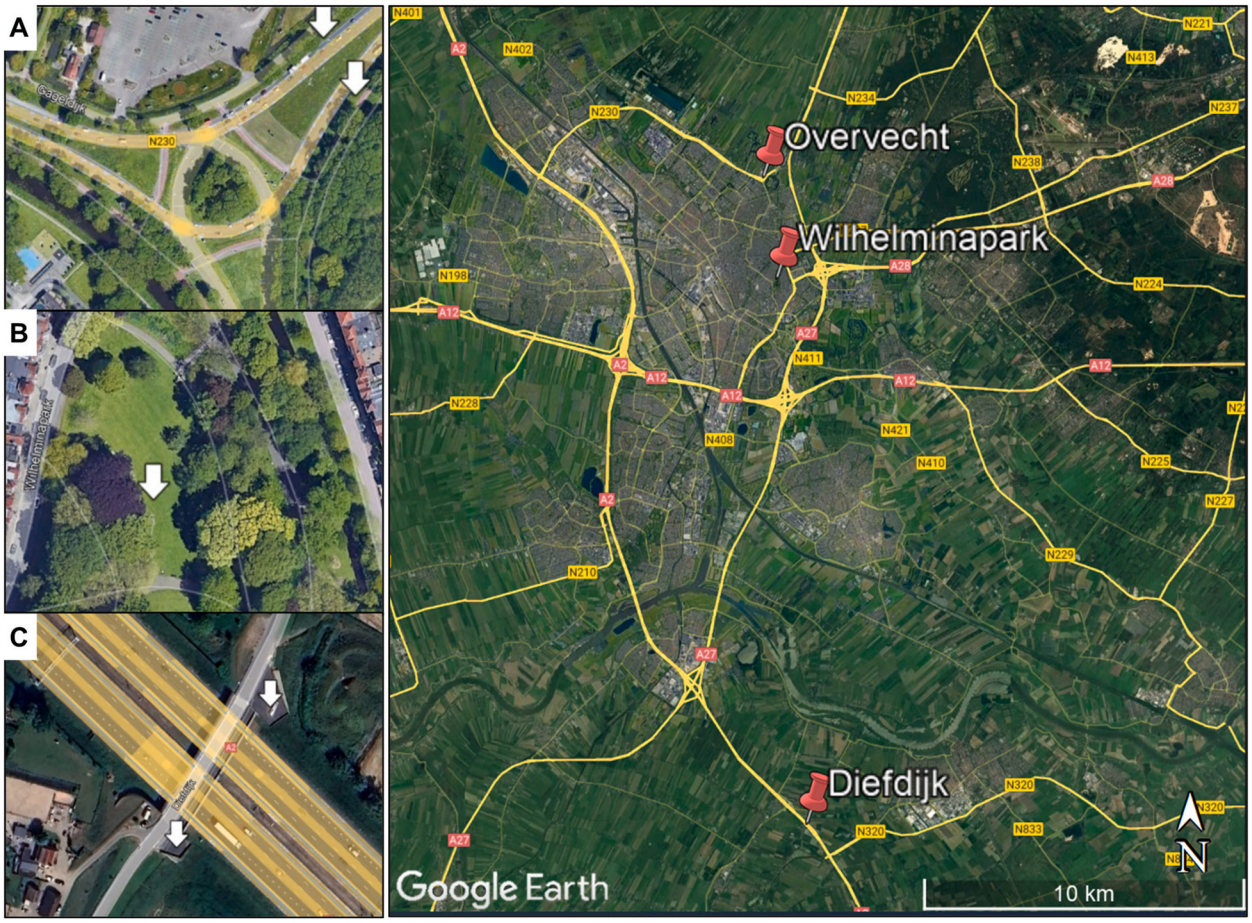

Fig. 1. Overview of sampling sites and equipment (white arrows) within and around Utrecht city, The Netherlands. Top to bottom: A) stop-and-go location nearby a roundabout (Overvecht), B) urban background location in a city park (Wilhelminapark) and C) highway/continuous traffic location (Diefdijk).

feasible duration with regards to the exposure study. More details on the analytical procedures can be found in our methods paper (Scibetta et al., in preparation) and supplemental text S1. Briefly, the extraction method was optimized to use of half of the large quartz filter from the Hivol sampler, instead of taking just a punch to make use of a large fraction of the sample mass. This was achieved by effectively concentrating the sample onto a smaller filter, which was inserted into a pyrolysis cup for further analysis. We additionally found that our laboratory gloves resulted in natural rubber contamination.

As part of the semi-experimental study, air sampling measurements were executed throughout the summers and autumns of 2022 and 2023. Since no electricity was available at the sampling sites, we used a gasoline generator to power the sampling equipment. To minimize exposure from the generator, we positioned it at least 50 m away from the sampling equipment, downwind and preferably behind some vegetation. Hourly weather conditions were collected and averages were calculated for the duration of each sampling campaign from the weather station at the Bilt, the Royal Netherlands Meteorological Institute (KNMI), located 3–18 km from the sites. We additionally collected 15-min average traffic counts once every hour to estimate the average hourly traffic (AHT) volume during the sessions. It was decided for volunteer convenience that the sessions should occur without rain, with wind speeds below 3 Beaufort (5.4 m/s), preferably between 11 a.m. and 3 p.m. An overview of the air samplers, types of filters used and the combination with subsequent analysis techniques can be found in Table 1.

2.2.1. Sampling- and analysis of rubber markers

A Hivol sampler (model TE-6070V equipped with TE-231 high-volume Cascade Impactor, Tisch Environmental, Cleves, OH) was used to sample PM_{10} on quartz microfiber sheets (20.3 × 25.4 cm, CAT No. 1851-865, Whatman™, Tisch Environmental) using a flowrate of 1.1 m^3/min. Afterward, in the research facility, the quartz sheets were carefully cut into two pieces using a customized metal cutting board (Supplement Fig. S2) and 90 %-ethanol cleaned Stainless Steel knife. Both halves were wrapped in plastic-free aluminum foil (CAT No. Z691577, Heathrow Scientific™, Fisher). Half of the filter was used for analysis by double-shot Py-GC-MS to determine the mass concentration TRWPs. The remaining half of the filter was used to analyze concentrations of selected trace metals and PAHs. We did not weigh the filters before and after sampling due to limitations in handling large filter sizes and to prevent contamination. Instead, a separate Harvard impactor at 10 L/min with a Teflon filter was used to measure PM_{10} mass concentrations.

2.2.1.1. Double-shot pyrolysis-gas chromatography-mass spectrometry analysis. The quantification of the mass of a selection of rubber markers was based on previously published protocols by Leslie et al (2022) and Brits et al. (2024), adapted for TRWPs (Brits et al., 2024; Leslie et al., 2022). The optimized protocol is described in detail in a methods paper (Scibetta et al., in preparation), summarized in supplement 10.3 (Text S1). Supplement Fig. S3 displays a graphical overview of the various steps involved in preparing and quantifying the rubber markers. Briefly, half of a quartz sheet was sonicated in methanol for 1-hr to extract particles from quartz filters. Sonication of quartz filters for analytical purposes is a well-established method and a common practice after PM collection for subsequent chemical analysis (Miljevic et al., 2014). The solvent was next filtrated over a 700 nm mesh sized, calcined quartz filter, to effectively concentrate the particles. A circular punch was taken out of the center of the filter and placed in a pyrolysis cup for further analysis using double-shot Py-GC-MS. Next, Py-GC-MS was used to quantify the thermal degradation products of the plastic particles present on the quartz punch. The natural- and synthetic polymers were quantified using a calibration curve made of pure standards of the polymers. Benzothiazole was quantified using cryo-milled rubber particles from 20 different tyres of various manufactures, as the pure rubber was not vulcanized (no sulfur present). More detail about the standards can be found in the paper from Scibetta et al. (in preparation). Internal standards were used for analysis control.

Supplement Table S2 displays the details for the indicator compounds used for quantification and their limit of detection (LOD) values. We quantified 4 different rubber markers as proxies for synthetic and natural rubber components of TRWPs. As indicator compounds for styrene-butadiene rubber, we included 3-cyclohexene-1-yl benzene (SBR Dimer) and 1-phenyl-3,4-divinyl-(1R,3trans,4trans)-Cyclohexane (SBR Trimer). Natural rubber indicator compounds were D-Limonene and 2,5,6-trimethyl-1,3,6-Heptatriene (NR Dimer2). In contrast to the indicator compounds used for TRWPs in previous studies and recommended by ISO protocols, we focused on dimer and trimer fragments due to their stronger specificity for rubber polymers (Panko et al., 2019). Moreover, they are more analytically stable than the traditional indicator compounds. Additionally, we quantified benzothiazole levels, as it is commonly used as a vulcanization accelerator in rubber tyres and remains the only marker currently used to assess toxicity in various in vitro and in vivo assays (Xu et al., 2024b; Zeng et al., 2016; Zhang et al., 2018). Next, we calculated the sum of NR D-Limonene and SBR Dimer ($\sum$(NR + SBR)) using their molarity. Moreover, method validation was conducted by assessing recoveries and variability of both pure standards and tyre particle mixtures. To ensure comparability between various measurements, calibration curves and sample measurements were normalized using polyfluorostyrene as the injection standard. Calibration curves R2 ranged between 0.98 to 0.99 for all markers used in the quantification. Recoveries were between 75 to 86 %, suggesting adequate though not fully quantitative recovery.

2.2.1.2. Quality assurance/quality control. Detailed QA/QC for the analytical procedures is presented in our methods paper (Scibetta et al., in preparation). Here we focus on the sampling procedures. To ensure minimal plastic contamination in sample preparation and sampling process, plastic products were avoided as much as feasible and alternative materials like stainless steel, glass, or aluminum were used whenever possible. 100 % Cotton laboratory coats were worn while working in the lab. Sample processing and preparation were performed in a laminar flow cabinet. All sampling heads were cleaned before each

Table 1
Overview of filters, samplers, analysis techniques used to measure tyre- and road wear particles and other traffic-related pollutants (parameters).

Filter material	Sampling head	Flowrate ($Lmin^{-1}$)	Analysis	Parameters
Quartz	Tisch high-volume sampler with PM_{10} inlet	1100	Double-shot Py-GC-MS	Mass synthetic & rubber polymer markers
			ICP-MS	Trace metals
			GC-MS	Polycyclic aromatic hydrocarbons
Teflon	Harvard PM_{10} Impactor	10	Gravimetric/reflectance	PM_{10}, reflectance
Real-time measurements	Testo DiscMini	1.0 ± 0.1	–	Ultrafine particle number
	microAeth® MA200/MA300	0.1		Black carbon

*__Abbreviations__: Py-GC-MS = pyrolysis-gas chromatography-mass spectrometry; ICP-MS = Inductively Coupled Plasma Mass Spectrometry; PM_{10} = Particulate matter with aerodynamic diameter <10 μm.

exposure day using ultrapure water and afterward rinsed extensively with 96 %-EtOH in the fume hood in a stainless-steel container. All filter holders were wrapped in plastic-free aluminum foil until sampling and during transport. The equipment was left overnight to dry in the fume hood. Prior to sampling, quartz sheets were baked in a muffle oven at 600 °C for 6-hrs (calcination; trap = 5 °C/min) to remove traces of polymers and other organic contaminants before sampling.

To quantify the potential contamination during the collection of the air samples, the transport and the handling of the filters in the laboratory, we collected an additional field blank filter during every sampling campaign. A field blank was defined as a filter treated similarly to the actual sample filter. The filter was put in the respective sampling head, wrapped in aluminum foil and transported to the sampling site. At the sampling site, the field blank filter holder was put without cover in the Hivol sampler until the air sampling would start, but not connected to an actual airflow. Just before the air sampling campaign started, the field blank filter was exchanged with the actual sample filter, again wrapped in aluminum foil and transported back to the laboratory. We additionally included lab blank filters, which were calcined, but did not leave the laboratory fume hoods. Further details can be found in supplement S1.

2.2.2. Other traffic-related air pollutants

Besides the release of TRWPs, traffic can also emit other exhaust- and non-exhaust air pollutants via combustion processes or brake-wear (Institute, 2022). To assess variability in exposure levels of TRWPs compared to other traffic-related air pollutants, we additionally quantified various combustion- and brake-wear-related components.

2.2.2.1. Trace metals and polycyclic aromatic hydrocarbons. Quartz PM_{10} filters from the Hivol samplers were analyzed by ICP-MS for trace elements of interest:

Cu, Fe, zinc (Zn), chromium (Cr), manganese (Mn), cadmium (Cd), lead (Pb), nickel (Ni), vanadium (V) and arsenic (As). Additionally, we measured the 16 EPA PAHs, including naphthalene, acenaphthylene, acenaphthene, fluorene, phenanthrene, anthracene, fluoranthene, pyrene, benzo(a)anthracene, chrysene, benzo(b+j)fluoranthene, benzo(k) fluoranthene, benzo(a)pyrene, indeno[1,2,3-cd]pyrene, dibenzo(a,h) anthracene and benzo(ghi)perylene. An extended table of the measured PAHs, their abbreviations and detection limits can be found in Supplement Table S3. Details on both analytical methods used for trace metals and PAHs determination are described elsewhere (Caricchia et al., 1999; Zanini et al., 2006). Extraction and analysis of PAH target compounds followed extraction EPA method 3545a, cleanup method EPA-3630 and analytical determination method EPA-8270D. A summary of the methods can be found in Supplement 11.4, Text S2.

Most of the trace elements and PAH levels were below the detection limit, defined as the average field blank value + 3 * standard deviation (SD) (Figure S5). We therefore decided only to include those PAHs and trace elements for which at least 50 % of the values were above the detection limit. These included indeno[1,2,3-cd]pyrene, V, Cr, Cu, Mn, Fe and As. As we hypothesized *a priori* that the park location would result in very low levels for most air pollutants, we applied this cut-off excluding the park location values. Supplemental Table S3 lists the trace elements and PAH pollutants included (green) or excluded from further assessment and characterization.

2.2.2.2. PM_{10} mass and reflectance. PM_{10} was sampled using Harvard Impactors (HI) operating at a flowrate of 10 L/min (Air Diagnostics and Engineering Inc, Harrison, ME, USA) on Teflon filters (37 mm, 2 mm pore size, PVC support ring, Pall, Port Washington, NY), following previously developed procedures (Eeftens et al., 2012). The sampling heads were covered in aluminum foil during transport and after sampling the HI were transported cooled back to the research facility. The flow was measured using calibrated rotameters 10 min after the start of the sampling and 10 min before the end of the campaign. Next, the elapsed-time from the pump units was combined with the flow rates to calculate sampled volumes. Nine filter field blanks were collected, rotating randomly over the three locations. Gravimetric and reflectance measurements on the Teflon filters were done according to the standard operating procedures of the ESCAPE study, described previously (Eeftens et al., 2012). Briefly, the particle mass of Teflon filters was determined by pre- and post-weighing the filters after 24-hr acclimatization in a climatized room (20–23 °C, 30–40 % humidity) using a Mettler MT5 microbalance (Mettler-Toledo, Greifensee, Switzerland) with a 1 μg precision. After post-weighing, the reflectance of all Teflon filters was determined at five spots using a Smoke Stain Reflectometer (model M43D; Diffusion Systems, London, UK). Next, the reflectance of the PM_{10} filters was transformed into absorption coefficients (a) using the following formula 1:

$$a = (A \ / \ 2V) * Ln(R_0 \ / \ R_s)$$

a = absorption coefficient (10^{-5}/m);
A = load filter area (m^2);
V = sampled volume (m^3);
R_0 = average reflectance of field blank filters;
R_s = reflectance of sampled filter (ISO, 1993).

The absorbance was calculated using the reflectance measurements and used as a proxy for elemental carbon (EC), as these measures have been shown to be highly correlated (Cyrys et al., 2003).

2.2.2.3. Real-time black carbon and ultrafine particle number concentrations. Real-time particle number concentrations were measured using a DiscMini Diffusion Charger (Testo, West Chester, USA). The DiscMini can monitor particles with a size cut-off between 10 to 300 nm, with concentrations between 10^3 to 10^6 pt/cm^3. The PNC measurements had a resolution of 1/second. Instruments were calibrated before each measurement and a zero check was performed before and after each campaign for 2 min, using a high-efficiency particulate air (HEPA) filter. Moreover, a microAeth®, either an MA200 or MA300, aethalometer (Aethlabs, San Francisco, USA) was used to monitor BC levels. BC was monitored with a time resolution of 60 s and a flow of 150 mL/min. A wavelength of >880 nm (infrared radiation) was interpreted as BC. Afterward, comparison measurements were performed, comparing the various aethalometer monitors, after which conversion factors were determined. The conversion factors were 1.14 and 1.20. More detailed information about the comparison campaign can be found in supplement 11.5.

2.3. Data management and analysis

Before interpreting the data, the quality of the measurements was assessed and data curation was executed. Rubber marker levels and benzothiazole signals were blank-corrected, using lab blanks from the dedicated MNP analytical laboratory at the Vrije Universiteit. The various markers were expressed as ng mass per cubic meter sampled air. We did not have a standard curve available to convert the benzothiazole signals to a mass concentration. Therefore, we divided the pyr-GC-MS intensity by the internal standard (ISTD: polyfluoro styrene, Polymer Source, 124 Rue Avro, Dorval, QC H9P 2X8, Canada) and converted the resultant unitless signal per cubic meter sampled air: $(AU/ISTD)^3/m^3$. The analytical LOD was determined as 3 times the SD of the average samples (n = 10), spiked with polymer standards at low concentrations.

One day it rained half of the day, resulting in missing data for the DiscMini (PNC), aethalometer (BC) and the filter for gravimetric and reflectance measurements ruptured. Additionally, on two other dates the PNC data was missing due to equipment failure. We estimated missing data points using size, hour and day-matched monitoring data from fixed-site monitors available via the National Air Quality

Monitoring Network in the neighborhood, accessed via https://data.rivm.nl/data/luchtmeetnet/. Respectively Kardinaal de Jongweg, Breukelen and Griftpark were used to estimate missing datapoints from the stop-and-go, highway and urban background (park) location. Next, we used ratios to calculate predicted concentrations. Missing data for BC were estimated using our own aethalometer data, as the reflectance and aethalometer measurements are generally highly correlated (Janssen et al., 2011). Hourly concentration data from ozone (O3) and nitrogen dioxide (NO2) were additionally collected from hourly- and daily matched monitoring data from fixed-site monitors. The PNC data were checked for device error codes including unreliable measurements based on flowrate and particle size using previously described procedures (Puustinen et al., 2007). On average, this procedure resulted in 1.7 to 18.4 % (SD = 5.3 %) deletion of datapoints, after which the data were aggregated to minute data. PM_{10}, PAH, trace element and absorbance data were field-blank corrected.

We compared distributions between the three sites and calculated ratios of the concentrations compared to the park location. We calculated Pearson correlations between the different rubber markers and with the other traffic-related air pollutants. To further help identify which of the tyre-, brake-wear or combustion-related air pollutants group together, we executed an explanatory factor analysis. The analysis included three factors and was executed with a varimax rotation method on the explanatory variables with pairwise comparisons The data analyses were performed using RStudio, version 4.2.3 (2023-03-15 UCRT).

3. Results

The distribution of measurement days per site and additional road and meteorological characteristics are listed in Table 2. In 2023, an additional 7 sampling measurements were conducted, in addition to the 16 planned sampling days, to increase statistical power. The final measurement campaign consisted of 23 sampling days, each lasting 4-hrs, executed between August–October 2022 and May–July 2023. On two of these days, sampling started 30–60 min earlier (10.30 a.m. instead of 11.30 a.m.), and on one day, we started 1 hr later (12:30 p.m.), due to the weather forecast predicting rain in the later afternoon or morning, respectively.

3.1. Atmospheric rubber marker blank levels and reproducibility

Fig. 2 shows the distribution of the atmospheric concentrations of NR and SBR markers, the ∑(NR + SBR) and benzothiazole, collected at the three measurement sites, compared with lab- and field blanks.

For all rubber components, the field blanks had higher levels compared to the lab blanks (Fig. 2). Field blanks did not differ systematically between locations, consistent with handling being the main source of contamination. The limit of detection calculated from the 23 field blanks (mean + 3*SD) was for SBR Dimer, SBR Trimer, NR Dimer2, NR D-Limonene and benzothiazole respectively: 8.44 ng/m^3, 14.1 ng/m^3, 7.33 ng/m^3, 4.7 ng/m^3 and 0.42 (AU/ISTD)^3/m^3 (Fig. 2, blue dashed line). Measurements collected in the park were above the analytical detection limit for most samples (Fig. 2, black line). However, natural rubber measurements collected in the park, were below the detection limit of the field blanks. For SBR Dimer and SBR Trimer respectively three (42.9 %) and two (28.6 %) of in total seven park samples, whereas for benzothiazole 5 of 7 samples (71.4 %) were above the average detection limit calculated from the 23 field blanks. Measurements at the two traffic sites were mostly above the detection limits.

The absolute differences and CV percentages of the three replicates can be found in Supplemental Table S4. All average CV scores were below 20 %, with 2-fold lower CV scores for SBR Dimer and benzothiazole, compared to the natural rubber markers and SBR Trimer.

3.2. Distributions of rubber markers and other air pollutants between locations

Distributions of all 4-hr average air pollutant concentrations and weather parameters can be found in Table 3, including mean ratios of concentrations between sites. The distributions of the rubber markers and key traffic-related components separated by site, can be found in Table 4, and for the other air pollutants in Table S5. The 4-hr average synthetic rubber concentrations ranged between 2.9 to 42.5 ng/m^3 for the dimer and 0.7 to 51.7 ng/m^3 for the trimer, with a median concentration of respectively 13.9 and 15.7 ng/m^3 (Fig. 2, Table 3). The natural rubber marker median levels were ~2-fold lower, with 7.2 ng/m^3 for the NR Dimer2, ranging between 1.9 to 29.1 ng/m^3, and 5.6 ng/m^3 for NR D-Limonene, ranging between 1.6 to 26.8 ng/m^3. Benzothiazole concentrations ranged between 0.2 to 7.7 AU/ISTD^3/m^3, with a median concentration of 1.0 (AU/ISTD)^3/m^3. On average, the lowest atmospheric natural and synthetic rubber concentrations were observed at the park location (3.1 to 5.1 ng/m^3), compared to both the highway (7.8 to 18.1 ng/m^3) and stop-and-go location (10.7 to 23.0 ng/m^3) (Fig. 2, Table 4) (See Table 5).

Compared to the park, the synthetic- and natural rubber levels were on average 2.4 and 2.6 times higher at the highway location. Slightly larger contrasts were observed for the stop-and-go location with 2.8 to 3.5 and 2.9 to 3.4 times higher synthetic- and natural rubber levels compared to the park (Table 3). Benzothiazole concentrations were 2.4-fold higher at the highway location and 4.6-fold higher at the stop-and-go location, compared to the park (Table 3). However, as the concentrations at the park were often below the detection limits of the field blanks, especially for natural rubber, these ratios should be interpreted with caution. Despite the lower traffic intensity, atmospheric rubber concentrations were 1.1–2.0 times higher for all rubber markers at the stop-and-go location compared to the highway (Tables 3 and 4).

Traffic-related trace elements with the largest contrasts between the stop-and-go and park location included the brake-wear-related elements Fe, Cr, Cu and Mn. Ratios ranged between 3.0 to 8.0x (SG:Park). Trace metal concentrations were higher at the stop-and-go location: 2.0 to 4.8x (SG:HW). BC and reflectance measurements, which could reflect both the non-exhaust and the exhaust component of traffic, were highest at

Table 2
Overview measurements campaigns and meteorological conditions at three traffic sites within and around Utrecht city.

Site	Year	Sampling days	AHT	Distance to:		Speed limit	RH	WS	Temp.
				Side of road	Road axis				
		(#)	(v/h)	(m)	(m)	(km/hr.)	(%)	(m/s)	(°C)
Stop-and-go	2022	3	3990	8	20	50	54.4 ± 14.3	4.0 ± 0.8	21.0 ± 4.4
	2023	6							
Highway	2022	3	9072	10	50	100	58.5 ± 17.8	3.6 ± 0.9	20.7 ± 3.0
	2023	4							
Urban background	2022	3	129	45	50	30	53.7 ± 21.0	4.7 ± 1.6	21.7 ± 5.5
	2023	4							

*Abbreviations: AHT = average hourly traffic count; v/h = vehicles per hour; RH = relative humidity; WS = windspeed; Temp. = temperature.

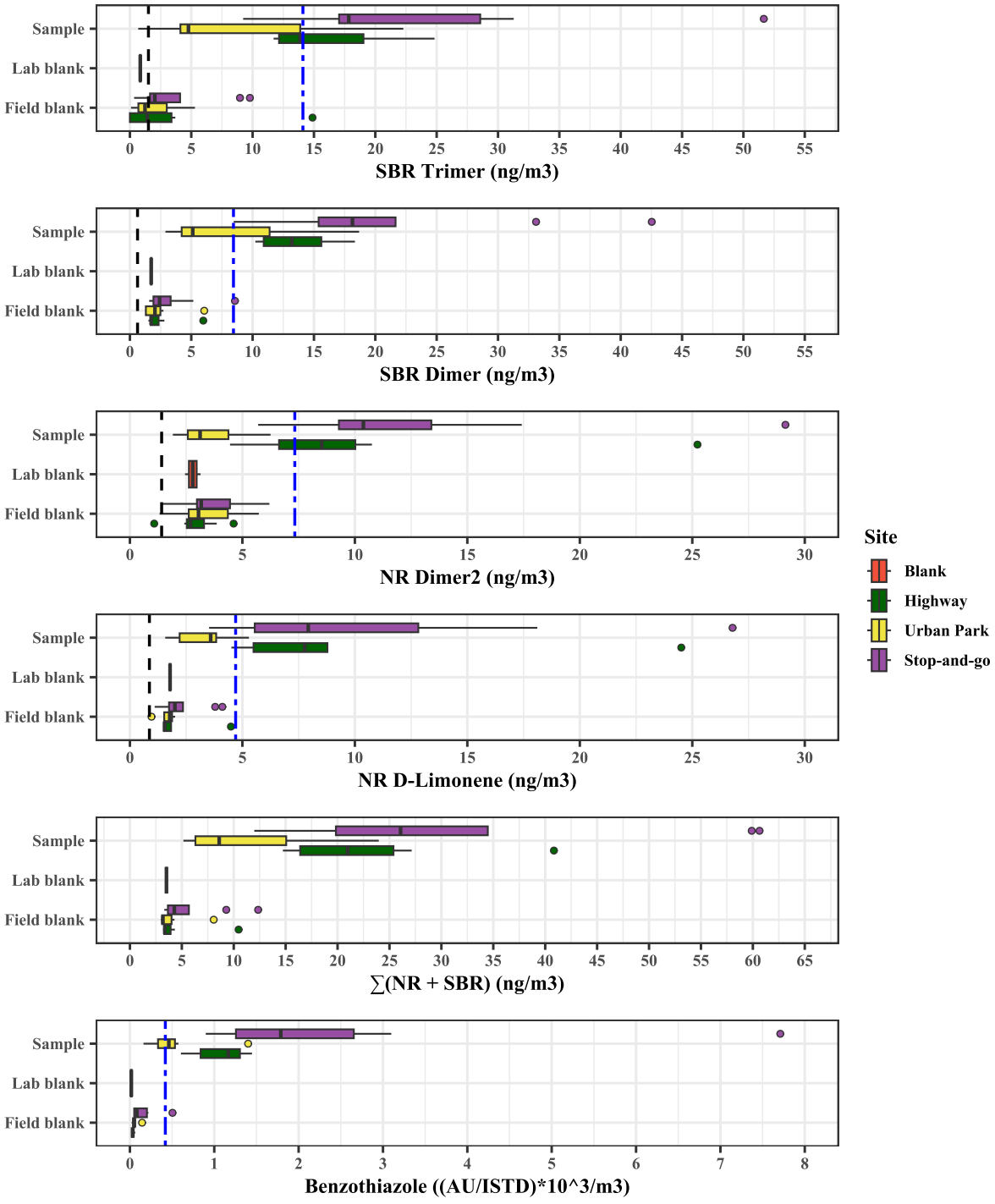

Fig. 2. Boxplots of atmospheric concentrations of natural (NR) and synthetic (SBR) markers, the sum of NR D-Limonene and SBR Dimer (∑(NR + SBR)) and benzothiazole, measured on sample, lab- and field blank filters (n = 23) collected at three different traffic sites. Dashed lines display analytical detection limits and dot-dashed lines in blue display the detection limits of the field blanks, calculated as mean + 3*SD.
Please note the different X-axis scales. (For interpretation of the references to colour in this figure legend, the reader is referred to the Web version of this article.)

Table 3
Distributions and ratios of 4-hr average measured air pollutant concentrations and weather parameters during measurement days (n = 23).

Variable	Unit	Mean	Median	SD	Min	Max	IQR	Ratio SG:P	Ratio HW:P	Ratio SG:HW
SBR Dimer	ng/m^3	14.9	13.9	9.1	2.9	42.5	8.7	2.8	2.0	1.4
SBR Trimer	ng/m^3	16.7	15.7	10.9	0.7	51.7	9.1	3.5	2.7	1.3
NR Dimer2	ng/m^3	9.2	7.2	6.9	1.9	29.1	5.8	3.4	2.6	1.3
NR D-Limonene	ng/m^3	8.0	5.6	6.7	1.6	26.8	4.9	2.9	2.6	1.1
∑(NR + SBR)	ng/m^3	22.9	19.8	14.9	5.2	60.6	13.0	2.8	2.2	1.3
Benzothiazole	$\left(\frac{AU}{ISTD}\right)^3/m^3$	1.4	1.0	1.7	0.2	7.7	0.9	4.6	2.4	2.0
PM_{10}	$\mu g/m^3$	24.7	25.0	11.0	11.1	52.6	13.8	1.1	0.7	1.7
BC	$\mu g/m^3$	1.12	1.06	0.63	0.28	2.44	0.66	2.3	1.3	1.8
Abs	m^{-5}	0.96	0.86	0.59	0.13	2.26	0.73	2.8	1.1	2.6
PNC	pt^{-3}/cm^3	11.2	10.7	5.6	3.4	24.5	5.5	1.3	1.1	1.2
V	ng/m^3	0.9	0.9	0.5	0.1	2.3	0.6	1.6	0.8	1.9
Cr	ng/m^3	3.9	2.8	3.9	0.4	15.7	3.5	5.2	1.7	3.1
Cu	ng/m^3	39.0	31.2	25.8	6.9	102.2	22.2	3.0	1.5	2.0
As	ng/m^3	0.2	0.2	0.2	0.0	0.9	0.2	1.4	0.7	1.9
Mn	ng/m^3	9.5	6.4	7.0	1.2	25.9	7.2	3.5	1.5	2.4
Fe	ng/m^3	728.7	327.7	756.1	84.8	2579.2	993.6	8.0	1.7	4.8
IP	ng/m^3	0.10	0.04	0.15	0.00	0.58	0.07	0.9	0.5	1.6
O_3[a]	$\mu g/m^3$	74.6	70.7	26.9	16.9	137.8	28.8	0.8	0.9	1.0
NO_2[a]	$\mu g/m^3$	11.8	10.5	6.6	3.4	31.0	6.8	1.4	2.1	0.7
Temperature	°C	21.1	21.1	4.2	14.4	28.6	5.7	1.0	1.0	1.0
Rel. humidity	%	55.8	56.6	16.9	23.0	81.4	20.8	1.1	1.0	1.1
Windspeed	m/s	4.1	4.0	1.1	2.2	7.0	1.3	0.8	0.9	0.9

*__Abbreviations:__ SBR = styrene-butadiene rubber; SBR Dimer = 3-cyclohexene-1-yl benzene; SBR Trimer = 1-phenyl-3,4-divinyl-, (1R,3trans,4trans)-Cyclohexane; NR = natural rubber; NR Dimer2 = 2,5-dimetyl-3-methylene-1,5-heptadiene; PM_{10} = particulate matter with an aerodynamic diameter <10 μm; Abs = absorbance; BC = black carbon; PNC = ultrafine particle number concentration; V = Vanadium; Cr = Chromium; Cu = Copper; As = Arsenic; Mn = Manganese; Fe = Iron; IP = Indeno[1,2,3-cd]pyrene; O_3 = ozone; NO_2 = nitrogen dioxide; IQR = interquartile range; SG = stop-and-go; P = park; HW = highway. [a]from https://data.rivm.nl/data/luchtmeetnet/.

Table 4
Median, minimum and maximum concentrations of 4-hr average rubber markers and selected other pollutants, separated by site. N = number of sampling days. Data of other air pollutants can be found in Supplement Table S5.

		SBR Dimer	SBR Trimer	NR Dimer2	NR D-Limonene	BZT
	n	ng/m^3	ng/m^3	ng/m^3	ng/m^3	$\left(\frac{AU}{ISTD}\right)^3/m^3$
Stop-and-go	9	18.1 (8.5; 42.5)	17.8 (9.2; 51.7)	10.4 (5.7; 29.1)	7.9 (3.5; 26.8)	1.8 (0.9; 7.7)
Highway	7	13.2 (10.2; 18.3)	13.9 (11.7; 24.8)	8.5 (4.5; 25.2)	7.8 (4.5; 24.5)	1.2 (0.6; 1.4)
Park	7	5.1 (2.9; 18.7)	4.8 (0.7; 22.3)	3.1 (1.9; 6.3)	3.6 (1.6; 5.3)	0.5 (0.2; 1.4)
		PM_{10} $\mu g/m^3$	Abs m^{-5}	PNC pt^a10^{-3}/cm^3	Fe ng/m^3	Cu ng/m^3
Stop-and-go	9	26.7 (11.6; 52.6)	1.4 (0.7; 2.3)	11.1 (4.0; 24.5)	1367.2 (646; 2579.2)	59.8 (26.8; 102.2)
Highway	7	15.3 (11.1; 33.2)	0.6 (0.2; 1.2)	11.4 (4.6; 12.7)	306.7 (202.4; 362.4)	29.7 (10.5; 42.3)
Park	7	26.3 (12.6; 38.4)	0.7 (0.1; 1)	9.9 (3.4; 20.8)	176.5 (84.8; 253.5)	20.5 (6.9; 37)

[a] **Abbreviations**: *SBR = styrene-butadiene rubber; SBR Dimer = 3-cyclohexene-1-yl benzene; SBR Trimer = 1-phenyl-3,4-divinyl-, (1R,3trans,4trans)-Cyclohexane; NR = natural rubber; NR Dimer2 = 2,5-dimetyl-3-methylene-1,5-heptadiene; BZT = benzothiazole;* PM_{10} = particulate matter <10 μm; Abs = absorbance; PNC = particle number concentration; Fe = Iron; Cu = Copper.

the stop-and-go location, with only small differences between the highway and park. PNC levels varied substantially, ranging between 3.4 to 24.5 pt^{-3}/cm^3. Small differences were observed between the various locations for PNC levels, with 10–30 % higher levels at the stop-and-go and highway locations compared to the park location. The only PAH in the current study with 50 % of concentrations above the variability of the field blank levels was Indeno[1,2,3-cd]pyrene (IP), which ranged between 0.00 to 0.58 ng/m^3 and was highest at the stop-and-go- and park location (Table 3).

3.3. Correlations between rubber markers and other major air pollutants

A Pearson correlation matrix with correlations of all air pollutants is presented in Fig. 3. Overall, we observed strong correlations within the same type of markers (i.e. natural-natural, or synthetic-synthetic), with values > 0.94. Correlations between synthetic- and natural rubber markers were moderately to strongly correlated with each other (r = 0.66 to 0.79). The correlations between the synthetic and natural rubber markers were very high (r > 0.94). This was also reflected in the high correlations between all individual rubber markers and the ∑(NR + SBR) (r > 0.89).

Table 5
Overview studies assessing tyre- and road wear PM_{10} concentrations and average contribution to PM_{10} levels. Extended table with additional descriptions and $PM_{2.5}$ measurements, can be found Supplement (Table S11).

Country	Sampling site	PM_{10} TRWP (ng/m^3)	Average contribution to PM_{10} (%)	Literature
Netherlands	Stop-and-go, highway, urban park (n = 23)	91.6 (20.6–242.6)	0.45 (0.07–1.48)	Current paper
Japan, USA, UK	Tunnels, highway, park, urban/rural etc. (n = 23)	920 (81–4480)	1.94	Panko et al. (2019)
Japan, USA, France	Hospital, park, rural, residential, industrial sites etc. (n = 89)	160 (NA; 1340)	0.84	Panko et al. (2013)
Japan	Highway (n = 1)	320	0.52	Unice et al. (2012)
China	Tunnel urban ring (n = 28)	6522±1455	4.7	Liu et al. (2023)
Republic of Korea	Bus stop (n = 24)	600–1800	5.5 (1.6–14.0)	Chae et al. (2024)
Norway	Marine (n = 7)	13.2–35.2	NA	Goßmann et al. (2023a)
Sweden	Marine (n = 3)	<LOD	NA	Goßmann et al. (2023b)
Japan	Urban (n = 2)	1.9–7.0	NA	Mizuguchi et al. (2023)

*__Abbreviations:__ USA = United States of America; UK = United Kingdom; TRWP = tyre- and road wear particles; PM_{10} = particulate matter with aerodynamic diameter <10 μm;.

The synthetic Dimer and Trimer were slightly higher correlated with absorbance and BC (r 0.63 to 0.69), compared to NR Dimer2 and NR D-Limonene (r 0.41 to 0.61). Furthermore, rubber markers were highly to moderately correlated with trace elements Cr > Fe > Mn > Cu (r 0.36 to 0.77) and had low correlations with V and As. Benzothiazole was highly correlated with all rubber markers, Abs, BC (r 0.69 to 0.72) and moderate to high with trace elements Fe, Cu, Cr, Mn and V (r 0.39 to 0.65). Low correlations were observed with the other major air pollutants PM_{10}, PNC, O_3, NO_2, IP and trace element As (r < 0.15). When analyzed by site, the Pearson correlations between rubber markers were similar for the site with the highest concentrations (Table S7). However, correlations with other components varied substantially across sites (Table S7–S9), partly related to the small number of samples per site.

The results of the three loadings of the exploratory factor analysis can be found in Supplement Table S6. The three factors explained together 67 % of the total variance. The first factor grouped all five rubber markers with partial loadings of BC, absorbance and trace elements Cr > Fe > Cu and Mn. The second factor predominantly represented absorbance (elemental carbon) and trace elements Mn > Fe > Cu > Cr > Cu > V. Synthetic rubber markers were also partially loaded on this factor (0.5), while the third factor included the remaining variables. Highest loadings for F3 included IP (0.9) followed by As, NO2, O3 and V.

4. Discussion

We characterized atmospheric levels of 4 synthetic- and natural rubber markers and benzothiazole, as proxies for TRWPs in atmospheric samples collected at three urban locations varying in traffic intensities. Compared to the park location, rubber concentrations were 2 to 5 times higher at the stop-and-go and highway locations. These contrasts were larger than those for combustion-related components PNC and PAH, but similar to BC and metals related to brake-wear (Fe, Mn, Cr and Cu). The rubber markers were highly correlated with each other and moderately to highly correlated with elemental carbon, BC and trace elements Fe, Mn, Cr and Cu. Our study contributes to the limited body of research on traffic-related MNPs in the atmospheric compartment.

4.1. Comparison with previous atmospheric rubber studies

Table S11 provides an overview of the limited number of studies that have quantified rubber TRWP concentrations in air using Py-GC-MS, listing the indicator compounds and reported TRWP concentrations. Large differences in measured rubber markers and calculated TRWPs were found. The most extensive studies were conducted by Panko et al. (2013; 2019) (Panko et al., 2013, 2019). They monitored the atmospheric mass of TRWPs in the $PM_{2.5}$-, and more limited, PM_{10} fraction at various roadside locations with different site characteristics, in three different countries.

Our finding of substantially higher rubber markers in PM_{10} at traffic sites agrees with previous studies (Table S11). In a study in France, rubber marker concentrations were much higher for roads with more than 25,000 vehicles/day, compared to less than 25,000 vehicles/day. Previous studies have noted that the increased friction of tyres on the road due to braking and cornering can result in higher non-exhaust levels compared to continuous driving, as seen on highways (Almeida et al., 2020). In the current study, we observed a higher number of vehicles of all types at the highway location compared to the stop-and-go and park locations. Nonetheless, the highest rubber exposure levels were recorded at the stop-and-go location, followed by the highway, with the lowest levels detected at the park. Consistent with our findings, Panko et al (2019) reported the highest $PM_{2.5}$ TRWP levels at the Blackwall Tunnel location in London (104 (30 to 290) ng/m^3) (Panko et al., 2019). The location was characterized by cars slowing down (braking), which probably resulted in the increased TRWP levels. The other location characterized by relatively higher exposure levels, but lower compared to the tunnel site, was Greenwich Blackheath (70 (20 to 270) ng/m^3), which was a highway location.

We detected rubber particles at the two traffic sites and the park location. In a small number of samples from the park location, exposure levels of synthetic rubber markers were higher than the LOD based on field blanks. This was corroborated by the benzothiazole marker, which was detected in 5 out of 7 samples from the park location. Panko et al (2019) also monitored an urban background location (n = 4, North Kensington), where 93 % of the $PM_{2.5}$ samples were above the LOD. Notably, rubber exposure levels were comparable to those at other roadside locations and even were among the top three highest levels monitored. However, the authors do note that the site was positioned next to a parking lot, meaning that they could not fully exclude local vehicular contributions. Additionally, a study focusing on e.g. TRWPs at sea, also observed exposure levels > LOD, albeit only in the larger size fractions (>PM_{10}) (Goßmann et al., 2023a). Although these results indeed confirm that traffic is the major contributor to rubber particles in the air, it also suggests that (urban) sites without direct local motorized-road vehicle contribution, can result in detectable TRWPs in the air. This is consistent with the relatively long atmospheric lifetime of $PM_{2.5}$, and to a lesser extent PM_{10}, resulting in source impacts at larger distances (Organization, 2021).

In contrast to our approach, Unice et al. (2012) explicitly excluded benzothiazole as a marker, arguing that it is not exclusively linked to tyre rubber. Instead, it is also found in antifreeze, corrosion inhibitors in paper production, dye production intermediates, and other sources (Unice et al., 2012). Consistently, we also did not use benzothiazole to

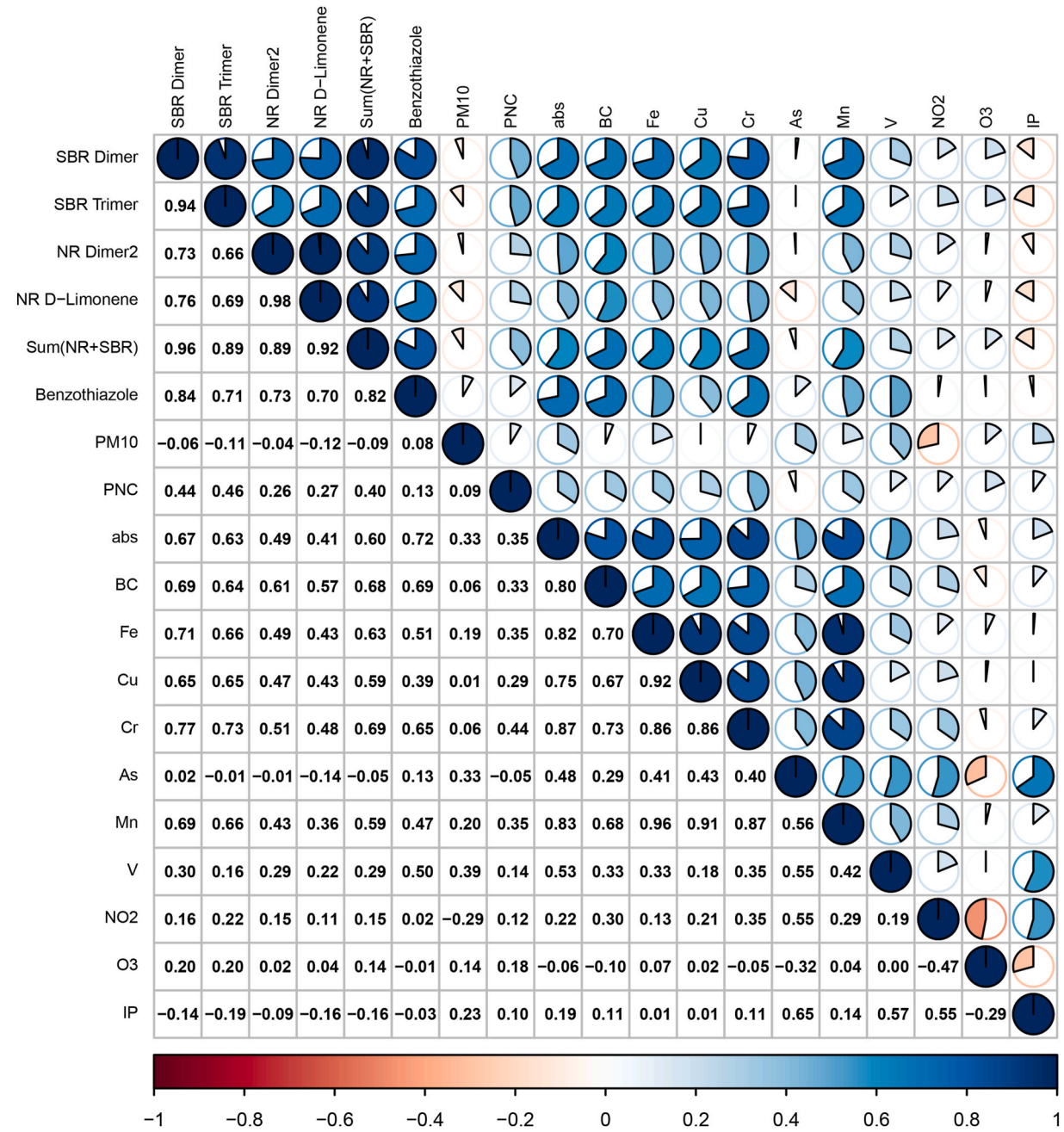

	SBR Dimer	SBR Trimer	NR Dimer2	NR D−Limonene	Sum(NR+SBR)	Benzothiazole	PM10	PNC	abs	BC	Fe	Cu	Cr	As	Mn	V	NO2	O3	IP
SBR Dimer																			
SBR Trimer	0.94																		
NR Dimer2	0.73	0.66																	
NR D−Limonene	0.76	0.69	0.98																
Sum(NR+SBR)	0.96	0.89	0.89	0.92															
Benzothiazole	0.84	0.71	0.73	0.70	0.82														
PM10	−0.06	−0.11	−0.04	−0.12	−0.09	0.08													
PNC	0.44	0.46	0.26	0.27	0.40	0.13	0.09												
abs	0.67	0.63	0.49	0.41	0.60	0.72	0.33	0.35											
BC	0.69	0.64	0.61	0.57	0.68	0.69	0.06	0.33	0.80										
Fe	0.71	0.66	0.49	0.43	0.63	0.51	0.19	0.35	0.82	0.70									
Cu	0.65	0.65	0.47	0.43	0.59	0.39	0.01	0.29	0.75	0.67	0.92								
Cr	0.77	0.73	0.51	0.48	0.69	0.65	0.06	0.44	0.87	0.73	0.86	0.86							
As	0.02	−0.01	−0.01	−0.14	−0.05	0.13	0.33	−0.05	0.48	0.29	0.41	0.43	0.40						
Mn	0.69	0.66	0.43	0.36	0.59	0.47	0.20	0.35	0.83	0.68	0.96	0.91	0.87	0.56					
V	0.30	0.16	0.29	0.22	0.29	0.50	0.39	0.14	0.53	0.33	0.33	0.18	0.35	0.55	0.42				
NO2	0.16	0.22	0.15	0.11	0.15	0.02	−0.29	0.12	0.22	0.30	0.13	0.21	0.35	0.55	0.29	0.19			
O3	0.20	0.20	0.02	0.04	0.14	−0.01	0.14	0.18	−0.06	−0.10	0.07	0.02	−0.05	−0.32	0.04	0.00	−0.47		
IP	−0.14	−0.19	−0.09	−0.16	−0.16	−0.03	0.23	0.10	0.19	0.11	0.01	0.01	0.11	0.65	0.14	0.57	0.55	−0.29	

Fig. 3. Pearson correlation matrix of concentrations of rubber markers and other air pollutants measured at the three measurement sites (n = 23). A figure of the scatterplots, density plots and the Pearson correlations of a part of the major air pollutants can be found in Fig. S6.
*__Abbreviations__: SBR = styrene-butadiene rubber; SBR Dimer = 3-cyclohexene-1-yl benzene; SBR Trimer = 1-phenyl-3,4-divinyl-, (1R,3trans, 4trans)-Cyclohexane; NR = natural rubber; NR Dimer2 = 2,5-dimetyl-3-methylene-1,5-heptadiene; BZT = benzothiazole; PM_{10} = particulate matter <10 μm; PNC = particle number concentration; Abs = absorbance; BC = black carbon; Fe = Iron; Cu = Copper; Cr = Chromium; As = Arsenic; Mn = Manganese; V = Vanadium; NO_2 = Nitrogen dioxide; O_3 = Ozone; IP = Indeno[1,2,3-cd]pyrene.

calculate TRWP mass levels, which was based upon the SBR Dimer and NR D-limonene markers. We did include benzothiazole as a separate marker of potential interest, because it (along with its derivatives) is widely used in epidemiological and toxicological hazard assessments, and has been correlated with a broad range of health endpoints (Liao et al., 2018; Xu et al., 2024b; Zeng et al., 2016). Moreover, as it is a common additive used for the vulcanization of rubber polymers, and given its high correlation with other rubber-specific markers in our samples, our findings suggest that, specifically in our setting, benzothiazole was related to TRWPs.

4.1.1. *Absolute TRWP levels and PM_{10} contribution*

The TRWP mass concentrations were calculated from the rubber markers following the ISO-method and calculations from previous studies (ISO, 2017; Liu et al., 2023; Panko et al., 2013; Panko et al., 2019; Unice et al., 2012). These calculations assume that the rubber distribution and subsequent contribution of rubber markers to individual TRWPs is homogeneous. Moreover, it assumes that tyres from different types of vehicles and brands have a similar contribution to the sum of SBR and NR. Consequently, we assumed that a tyre exists for 50 % out of ∑(NR + SBR), whereas TRWPs exist out of 25 % rubber polymers, due to the additional mixing with road debris, brake- and

pavement wear (Panko et al., 2019). However, the contribution of rubber to TRWPs is potentially highly variable, due to variances in analytical techniques (e.g. indicator compounds used, double-shot) and the high variation in the contribution of various rubber markers to different types- and brands of tyres (Jeong et al., 2024). Recent findings by Jeong et al (2024) revealed substantial variation in the ratios of SBR + BR and NR across different tyre types, including passenger car, lightweight truck- and heavy truck tyres (Jeong et al., 2024). Weight concentrations varied between 3.8 to 29.9 % for SBR and 5.6 to 67.0 % for NR for all types of tyres. Passenger car tyres had on average 2.8 times higher SBR levels, compared to NR, whereas for heavyweight trucks this difference was on average 0.3 times. Indicating that the use of a single estimate might not capture the diversity of rubber compositions in real-world tyres. Nonetheless, by applying a constant 25 % polymer content for the calculations, we aimed to provide a standardized reference to allow for comparisons with previous studies:

We found an average TRWP content of 91.6 (20.6 to 242.6) ng/m^3. This represented an average PM_{10} mass contribution of 0.45 (0.07 to 1.48)%. Compared to the park, TRWP mass contributions were higher at the stop-and-go- and highway locations (PM_{10} TRWPs SG and HW = 0.51 %, P = 0.13 %). We additionally estimated the TRWP levels and PM_{10} mass contribution based on the SBR and NR ratios in various tyre types, according to Jeong et al (2024) (Jeong et al., 2024). The calculations can be found in Supplemental Text 11.5 and Table S12–S13. Calculations for the other studies, using 25 % polymer content in TRWPs, are shown in Table S11. TRWP levels ranged between 81 to 4480 ng/m^3 and 4 to 7977 ng/m^3 within the PM_{10} and $PM_{2.5}$ fraction, respectively (Chae et al., 2024; Liu et al., 2023; Panko et al., 2013, 2019; Unice et al., 2012). Generally, higher $PM_{2.5}$ concentrations were observed near a bus stop and with tunnel measurements. There is therefore significant uncertainty in absolute levels, particularly across environments. Mass contributions ranged from 0.52 to 1.94 % for PM_{10} and 0.23 to 14.0 % for $PM_{2.5}$. This overview documents substantial variability of percentage contributions to PM across studies.

Our findings are on the lower end of the range of those reported in previous studies. Differences between studies can be due to analytical differences, environmental factors, road- and site characteristics and the specific timing of the often relatively short sampling campaigns. Our sampling was purposefully conducted between the morning and afternoon traffic jams. Furthermore, TRWP levels varied widely throughout the year (Geisler et al., 1974; Liu et al., 2023), indicating that levels may vary seasonally. Moreover, we noticed that for multiple studies the TRWP exposure levels within the $PM_{2.5}$ size range could not be estimated as they were below the detection limit (Goßmann et al., 2023a, 2023b; Mizuguchi et al., 2023; Panko et al., 2019). This was in line with the TRWP mass contributions, which were higher within the PM_{10}, compared to the $PM_{2.5}$ size fraction (Panko et al., 2019). This is consistent with TRWPs primarily contributing to the coarse size range. Consistently, there is a relatively large body of literature documenting TRWP levels in road dust and run-off (Baensch-Baltruschat et al., 2020; Khan et al., 2024; Vollertsen, 2018).

The large variability across studies suggests we should be very cautious about interpreting the absolute TRWP exposure levels and subsequent PM mass contributions (Jeong et al., 2024). Modeling approaches or abrasion studies generally estimate the contribution of TRWP mass to $PM_{2.5}$ and PM_{10} an order of magnitude higher: between 1 to 4 % and 3 to 8 %, respectively (Kole et al., 2017; Tonegawa et al., 2021). The uncertainty partly arises from the variability in polymer mass contribution across different tyres and partly from the highly variable inclusion of brake wear, road debris, and pavement wear in TRWPs. Furthermore, since local sources account for ~23 % of PM_{10} concentrations when comparing urban background areas with street sites across Europe, the remaining PM_{10} mass is primarily influenced by long-range transport processes (Eeftens et al., 2012).

4.2. Rubber markers in relation to other traffic-related air pollutants

For the rubber markers, levels between the stop-and-go and highway locations varied between 1.1 to 2.0 times and between stop-and-go and park locations between 2.8 to 4.6 times (Table 3). These contrasts were similar to contrasts in BC and brake-wear related trace elements, with the exception of Fe (Table 3). Furthermore, we observed relatively high correlations between the rubber markers and absorbance, BC and traffic-related trace elements (Fig. 3).

BC is used as a reinforcing agent (filler, 22 to 40 %) in tyres to increase tensile strength and UV-resistance and has been observed in atmospheric TRWP samples (Kole et al., 2017; Strak et al., 2011). Additionally, BC is formed through incomplete combustion of fuels. The measured BC in our air samples could therefore have multiple sources, including tyre wear, emissions from diesel engines, residential heating or even industrial processes. Furthermore, especially at the stop-and-go location the cars had to wait minutes in front of a traffic-light, potentially contributing to an increase in specifically the exhaust fraction. Noticeably, in contrast to our study, Panko et al (2019) did not observe significant correlations between TRWPs in $PM_{2.5}$ and pollutants NO and BC (Panko et al., 2019). Given the source, we consider positive correlations between rubber markers and BC plausible.

Several studies analyzing SEM images of TRWPs have observed black, sausage-like particles with elemental crustations, suggesting a potential strong correlation between BC, trace elements and rubber markers (Rausch et al., 2022). Fe, as one of the most abundant heavy metals associated with atmospheric traffic-related PM_{10}, originates from various sources including brake wear, resuspension dust and direct tailpipe emissions (Gietl et al., 2010; Thorpe et al., 2008). As the cars at the stop-and-go location had to repeatedly brake and wait for a traffic light, this might explain the larger contrast observed for Fe, compared to the other air pollutants (Boogaard et al., 2011; Gietl et al., 2010). Cr and Cu are released from the organic brake pads and steel disc brakes. Other trace metals that have been reported, mainly associated with tyre wear, included Zn, Mn, barium, kalium, tin, antimony and titanium (Kwak et al., 2013; Thorpe et al., 2008). A study assessing TRWP road dust concentrations in eight megacities in China, additionally looked at correlations between TRWP markers and trace elements (Sun et al., 2022). They also observed high correlations between rubber markers and sulfur, Fe, Mn, calcium, kalium and titanium, but a low correlation with Zn. This might confirm that Zn is not a suitable marker for TRWPs.

4.3. Strengths and limitations

In this paper, we quantified the mass of synthetic and natural rubber using various indicator compounds as proxies. The most abundant tyre rubber markers quantified include styrene, dipentene, butadiene and vinyl-cyclohexene, some of them compliant with the ISO standards (ISO, 2017). Previous studies have expressed concerns regarding the uniqueness and reproducibility of the different indicator compounds (Seeley et al., 2023; Unice et al., 2012). A major strength in this regard, was the addition of double-shot to the Py-GC-MS method. Organic compounds are known to interfere with the analysis, especially for trimer markers. Due to the double heating step, as described by Brits et al (2024), the volatile organic compounds are first released in the thermal desorption step (Brits et al., 2024). Additionally, we purposefully choose different indicator compounds, as these are more stable throughout the double-shot Py-GC-MS analyses.

To address the high risk of potential contamination, we incorporated a relative large number of field blanks and implemented additional measures to limit contamination. For quality control of the analytical procedure, we collected additional filters to determine the variability from sample handling, analytical procedures and splitting a filter into two halves. All rubber markers had relatively low CV scores, indicating good repeatability of measurements. Additionally, both external calibration analysis and internal standards were used during the analytical

procedure to increase the reliability and reproducibility of quantitative assessment.

We observed generally higher correlations between synthetic rubber markers with brake-wear and primary air pollutants, compared to NR markers (Fig. 3). Furthermore, the scatterplots in Supplemental Fig. S6 showed generally greater variability associated with NR markers compared to the SBR markers. Additionally, the higher CV values for both NR markers, compared to SBR Dimer and benzothiazole (Table S4). Taken together, this might suggest greater imprecision and variability in the measurements of NR markers relative to the SBR markers.

A major strength of our paper was its focus on PM_{10}-size-range TRWPs, as multiple studies focusing on smaller size ranges did not reach the LOD. Although TRWPs are currently a relatively small fraction of total PM exposure, their relative proportion is expected to increase as tailpipe emissions further decrease. Additionally, we expect absolute levels may increase due to additional friction from heavier electric vehicles, which was also in line with the measurements performed by Chae et al. (2024) (Chae et al., 2024; Jiang et al., 2022). Furthermore, by including both roadside and urban background locations, we broadened the context of our study, allowing for a more comprehensive comparison across varied environments. Focusing on specific times and weather conditions, might have limited the representativeness of the results. E.g. Higher levels of TRWPs have been observed in winter. However, as we conducted sampling in parallel with volunteer visits to the sites, sampling was constrained by practical considerations, particularly the comfort and availability of the volunteers during different seasons. Nonetheless, despite the limitations in sample size and seasonal variation, we believe our study makes a valuable contribution to the limited number of measurements currently available within literature.

A major limitation in our and previous studies is the calculation of absolute concentrations of TRWPs based on the measured rubber markers. The selection of markers for TRWP quantification in this study was based on a rigorous screening process. Pure SBR and isoprene rubber (IR), as defined by the ISO 20539 methodology, along with natural rubber (NR), were analyzed using py-GC-MS in full-scan mode to identify all potential markers (ISO, 2017). The initial set of markers was then refined by comparing them to pyrolysis byproducts of various plastic polymers to ensure the specificity of the selected TRWP markers. Additionally, the shortlisted markers were further evaluated against those produced by the pyrolysis of tyre particles, allowing for the identification and exclusion of potential matrix interferences. As a result of this systematic selection process, these three final markers (D-limonene, SBR dimer, and benzothiazole) were identified as the most suitable for the quantification of TRWPs in air samples. We acknowledge however, that uncertainty remains in this area.

5. Conclusion

This study quantified exposure to traffic-related rubber MNPs in atmospheric samples in urban settings, adding to the limited knowledge available in the peer-reviewed literature. Compared to an urban background location, we observed a 2.6 to 4.6-fold increase in the mass of rubber marker levels, indicative of increased TRWPs nearby major roads. Moderate to high correlations were observed with BC and brake-wear components. The TRWP measurements provide a good basis for assessing associations with health outcomes in the related health study.

Funding sources

This work was supported by the European Union's Horizon 2020 research and innovation program project Polyrisk [grant agreement No. 964766].

CRediT authorship contribution statement

E.S. Lenssen: Writing – review & editing, Writing – original draft, Visualization, Resources, Methodology, Investigation, Formal analysis, Conceptualization. **L. Scibetta:** Writing – review & editing, Methodology, Investigation. **M. Brits:** Writing – review & editing, Investigation. **M. Lamoree:** Writing – review & editing, Methodology. **L. Caiazzo:** Writing – review & editing, Investigation. **M.R. Montereali:** Writing – review & editing, Investigation. **S. Manzo:** Writing – review & editing, Investigation. **S. Chiavarini:** Writing – review & editing, Investigation. **R. Vermeulen:** Writing – review & editing. **R.H.H. Pieters:** Writing – review & editing, Supervision, Funding acquisition, Conceptualization. **G. Hoek:** Writing – review & editing, Supervision, Conceptualization.

Declaration of competing interest

The authors declare that they have no known competing financial interests or personal relationships that could have appeared to influence the work reported in this paper.

Acknowledgements

We would like to thank all the volunteers for their participation and enthusiasm. Moreover, we would like to thank Isabella van Schothorst, Stavri Karasiali, Laura Torroba Vicario, Fleur Froeling and Kees Meliefste for their invaluable support and flexibility in setting up the air quality measurement equipment and for undertaking the heavy lifting required to set up the rest of the campaign equipment.

Appendix A. Supplementary data

Supplementary data to this article can be found online at https://doi.org/10.1016/j.atmosenv.2025.121257.

Data availability

Data will be made available on request.

References

Allegretta, I., et al., 2022. *SEM-EDX hyperspectral data analysis for the study of soil aggregates.* Geoderma, 406, 115540.
Almeida, S.M., et al., 2020. Ambient particulate matter source apportionment using receptor modelling in European and Central Asia urban areas. Environ. Pollut. 266, 115199.
Amato, F., et al., 2020. OECD publ. Non-Exhaust Particulate Emissions from Road Transport: an Ignored Environmental Policy Challenge. France, Paris.
Andersson-Sköld, Y., et al., 2020. Microplastics from tyre and road wear: a literature review, pp. 1–131. VTI rapport 1028A. 2018/0038-7.2.
Baensch-Baltruschat, B., et al., 2020. Tyre and road wear particles (TRWP)-A review of generation, properties, emissions, human health risk, ecotoxicity, and fate in the environment. Science of the total Environment, 733, 137823.
Beji, A., et al., 2020. Non-exhaust particle emissions under various driving conditions: implications for sustainable mobility. Transport. Res. Transport Environ. 81, 102290.
Blomqvist, G., et al., 2023. Microplastics in snow in urban traffic environments. Statens väg-och transportforskningsinstitut, pp. 1–81. VTI rapport 1171A. 2021/0411-7.2.
Boogaard, H., et al., 2011. Contrast in air pollution components between major streets and background locations: particulate matter mass, black carbon, elemental composition, nitrogen oxide and ultrafine particle number. Atmos. Environ. 45 (3), 650–658.
Brits, M., et al., 2024. Quantitation of micro and nanoplastics in human blood by pyrolysis-gas chromatography–mass spectrometry. Microplast. Nanoplast. 4 (1), 12.
Browne, M.A., Galloway, T., Thompson, R., 2007. Microplastic—an emerging contaminant of potential concern? Integrated Environmental Assessment and Management. Int. J. 3 (4), 559–561.
Caricchia, A.M., Chiavarini, S., Pezza, M., 1999. Polycyclic aromatic hydrocarbons in the urban atmospheric particulate matter in the city of Naples (Italy). Atmos. Environ. 33 (23), 3731–3738.
Celeiro, M., et al., 2021. Evaluation of chemicals of environmental concern in crumb rubber and water leachates from several types of synthetic turf football pitches. Chemosphere 270, 128610.
Chae, E., Jung, U., Choi, S.-S., 2024. Seasonal variations in concentrations of PM2. 5 and tire wear particle of< 2.5 μm (TWP2. 5) and polymeric components of PM2. 5 at a bus stop. Atmos. Environ. 318, 120243.
Cyrys, J., et al., 2003. Comparison between different traffic-related particle indicators: elemental carbon (EC), PM2. 5 mass, and absorbance. Journal of Exposure Science & Environmental Epidemiology, 13 (2), 134–143.

Dall'Osto, M., et al., 2014. Characteristics of tyre dust in polluted air: studies by single particle mass spectrometry (ATOFMS). Atmos. Environ. 94, 224–230.
Denier van der Gon, H.A., et al., 2013. The policy relevance of wear emissions from road transport, now and in the future—an international workshop report and consensus statement. Journal of the Air & Waste Management Association, 63 (2), 136–149.
Dris, R., et al., 2015. Microplastic contamination in an urban area: a case study in Greater Paris. Environ. Chem. 12 (5), 592–599.
Eeftens, M., et al., 2012. Spatial variation of PM2. 5, PM10, PM2. 5 absorbance and PMcoarse concentrations between and within 20 European study areas and the relationship with NO2–results of the ESCAPE project. Atmos. Environ. 62, 303–317.
Eisentraut, P., et al., 2018. Two birds with one stone—fast and simultaneous analysis of microplastics: microparticles derived from thermoplastics and tire wear. Environmental Science & Technology Letters, 5 (10), 608–613.
Fomba, K.W., et al., 2018. Assessment of trace metal levels in size-resolved particulate matter in the area of Leipzig. Atmos. Environ. 176, 60–70.
Geisler, F.H., et al., 1974. Deuterium micromapping of biological samples by using the D (T,n)4He reaction and plastic track detectors. Science 186 (4161), 361–363.
Gietl, J.K., et al., 2010. Identification of brake wear particles and derivation of a quantitative tracer for brake dust at a major road. Atmos. Environ. 44 (2), 141–146.
Gouveia, N., Maisonet, M., 2006. Health effects of air pollution: an overview. Air quality guidelines: global update 2005. Particulat. Matter., Ozone, Nitrogen Dioxide Sulfur Dioxide 87–109.
Goßmann, I., et al., 2023a. Occurrence and backtracking of microplastic mass loads including tire wear particles in northern Atlantic air. Nat. Commun. 14 (1), 3707.
Goßmann, I., et al., 2023b. Unraveling the marine microplastic cycle: the first simultaneous data set for air, sea surface microlayer, and underlying water. Environmental science & technology, 57 (43), 16541–16551.
Institute, H.E., 2022. Systematic review and meta-analysis of selected health effects of long-term exposure to traffic-related air pollution. HEI Special Rep. 23.
Iso, I., 1993. 9835, Ambient Air–Determination of a Black Smoke index. Geneva: International Organization for Standardization.
Iso, I., 2017. *TS 20593: Ambient air-Determination of the Mass Concentration of Tire and Road Wear Particles (TRWP)-Pyrolysis-GC-MS Method.* International Organization for Standardization. Switzerland, Geneve.
Jaikumar, G., et al., 2019. Reproductive toxicity of primary and secondary microplastics to three cladocerans during chronic exposure. Environ. Pollut. 249, 638–646.
Janssen, N.A., et al., 2011. Black carbon as an additional indicator of the adverse health effects of airborne particles compared with PM10 and PM2. 5. Environmental health perspectives, 119 (12), 1691–1699.
Järlskog, I., et al., 2022. Concentrations of tire wear microplastics and other traffic-derived non-exhaust particles in the road environment. Environment international 170, 107618.
Jeong, S., et al., 2024. Quantification of tire wear particles in road dust based on synthetic/natural rubber ratio using pyrolysis-gas chromatography–mass spectrometry across diverse tire types. Sci. Total Environ., 173796
Jiang, R., et al., 2022. Exhaust and non-exhaust airborne particles from diesel and electric buses in Xi'an: a comparative analysis. Chemosphere 306, 135523.
Khan, F.R., et al., 2024. An overview of the key topics related to the study of tire particles and their chemical leachates: from problems to solutions. TrAC, Trends Anal. Chem., 117563
Kole, P.J., et al., 2017. Wear and tear of tyres: a stealthy source of microplastics in the environment. Int. J. Environ. Res. Publ. Health 14 (10).
Kwak, J.h, et al., 2013. Characterization of non-exhaust coarse and fine particles from on-road driving and laboratory measurements. Sci. Total Environ. 458, 273–282.
Leslie, H.A., et al., 2022. Discovery and quantification of plastic particle pollution in human blood. Environment international 163, 107199.
Liao, C., Kim, U.-J., Kannan, K., 2018. A review of environmental occurrence, fate, exposure, and toxicity of benzothiazoles. Environ. Sci. Technol. 52 (9), 5007–5026.
Liu, M., et al., 2023. Chemical composition and potential health risks of tire and road wear microplastics from light-duty vehicles in an urban tunnel in China. Environ. Pollut. 330, 121835.
Lough, G.C., et al., 2005. Emissions of metals associated with motor vehicle roadways. Environmental science & technology, 39 (3), 826–836.
Maurizi, L., et al., 2024. Every breath you take: high concentration of breathable microplastics in indoor environments. Chemosphere, 142553.
Mennekes, D., Nowack, B., 2022. Tire wear particle emissions: measurement data where are you? Sci. Total Environ. 830, 154655.
Miljevic, B., et al., 2014. To sonicate or not to sonicate PM filters: reactive oxygen species generation upon ultrasonic irradiation. Aerosol. Sci. Technol. 48 (12), 1276–1284.
Mizuguchi, H., et al., 2023. Direct analysis of airborne microplastics collected on quartz filters by pyrolysis-gas chromatography/mass spectrometry. Journal of Analytical and Applied Pyrolysis, 171, 105946.
Müller, A., et al., 2022. Determination of tire wear markers in soil samples and their distribution in a roadside soil. Chemosphere 294, 133653.
Nafea, T.H., et al., 2024. Microplastics Aloft: a comprehensive exploration of sources, transport, variations, interactions and their implications on human health in the atmospheric realm. Earth Sci. Rev., 104864
Organization, W.H., 2021. WHO Global Air Quality Guidelines: Particulate Matter (PM2. 5 and PM10), Ozone, Nitrogen Dioxide, Sulfur Dioxide and Carbon Monoxide. World Health Organization.
Panko, J.M., et al., 2013. Measurement of airborne concentrations of tire and road wear particles in urban and rural areas of France, Japan, and the United States. Atmos. Environ. 72, 192–199.
Panko, J.M., et al., 2019. Evaluation of tire wear contribution to pm2. 5 in urban environments. Atmosphere 10 (2), 99.
Park, I., Kim, H., Lee, S., 2018. Characteristics of tire wear particles generated in a laboratory simulation of tire/road contact conditions. J. Aerosol Sci. 124, 30–40.
Piscitello, A., et al., 2021. *Non-exhaust traffic emissions: sources, characterization, and mitigation measures.* Science of the Total Environment, 766, 144440.
Puustinen, A., et al., 2007. Spatial variation of particle number and mass over four European cities. Atmos. Environ. 41 (31), 6622–6636.
Quik, J.T.K., H, A., Steenmeijer, M.A., Mellink, Y., van Bruggen, A., 2024. Rijksinstituut voor Volksgezondheid en Milieu RIVM. Emission of Microplastics to Water, Soil, and Air. What can we do about it? 190.
Rausch, J., et al., 2022. Automated identification and quantification of tire wear particles (TWP) in airborne dust: SEM/EDX single particle analysis coupled to a machine learning classifier. Science of the Total Environment, 803, 149832.
Schauer, J., 2006. Characterization of Metals Emitted from Motor Vehicles. Research Report (Health Effects Institute), pp. 1–76, 2006 Mar(133).
Seeley, M.E., Lynch, J.M., 2023. Previous successes and untapped potential of pyrolysis–GC/MS for the analysis of plastic pollution. Analyt. Bioanalytic. Chem. 415 (15), 2873–2890.
Snijder, L., Nusselder, S., 2019. Plasticgebruik en verwerking van plastic afval in Nederland, 19.2T13.026. CE Delft, pp. 1–55.
Strak, M., et al., 2011. Variation in characteristics of ambient particulate matter at eight locations in The Netherlands–The RAPTES project. Atmos. Environ. 45 (26), 4442–4453.
Strak, M., et al., 2012. Respiratory health effects of airborne particulate matter: the role of particle size, composition, and oxidative potential—the RAPTES project. Environmental health perspectives, 120 (8), 1183–1189.
Sun, J., et al., 2022. Explorations of tire and road wear microplastics in road dust PM2. 5 at eight megacities in China. Science of the Total Environment, 823, 153717.
Svensson, N., et al., 2023. Effects of a porous asphalt pavement on dust suspension and PM10 concentration. Transport. Res. Transport Environ. 123, 103921.
Thorpe, A., Harrison, R.M., 2008. Sources and properties of non-exhaust particulate matter from road traffic: a review. Science of the total environment, 400 (1–3), 270–282.
Tonegawa, Y., Sasaki, S., 2021. Development of tire-wear particle emission measurements for passenger vehicles. Emission Control Science and Technology, 7, 56–62.
Unice, K.M., Kreider, M.L., Panko, J.M., 2012. Use of a deuterated internal standard with pyrolysis-GC/MS dimeric marker analysis to quantify tire tread particles in the environment. International Journal of Environmental Research and Public Health, 9 (11), 4033–4055.
van Broekhuizen, P., 2022. CASE STUDY ON THE IMPACT OF THE RGF IN DUTCH INDUSTRIES 'PILOT RUBBER TYRES' Airborne release of tyre wear particles, pp. 1–79. www.nanorigo.nl.
Verschoor, A., et al., 2016. Emission of microplastics and potential mitigation measures: Abrasive cleaning agents, paints and tyre wear. RIVM Report 2016-0026 1–76.
Vollertsen, J., 2018. Review of available measurements of organic micropollutants, microplastics and associated substances in road run-off. Microproof deliverable 6, 1–18.
Wang, Y.-L., et al., 2020. Potent impact of plastic nanomaterials and micromaterials on the food chain and human health. International journal of molecular sciences, 21 (5), 1727.
Wright, S.L., Kelly, F.J., 2017. Plastic and human health: a micro issue? Environ. Sci. Technol. 51 (12), 6634–6647.
Xu, L., et al., 2024a. Characterization of atmospheric microplastics in Hangzhou, a megacity of the Yangtze river delta, China. Environmental Science: Atmospheres 4 (10), 1161–1169.
Xu, X., et al., 2024b. Synthesis and biological evaluation of novel benzothiazole derivatives as potential anticancer and antiinflammatory agents. Front. Chem. 12, 1384301.
Zanini, G., et al., 2006. Concentration measurement in a road tunnel as a method to assess "real-world" vehicles exhaust emissions. Atmos. Environ. 40 (7), 1242–1254.
Zeng, F., Sherry, J.P., Bols, N.C., 2016. Evaluating the toxic potential of benzothiazoles with the rainbow trout cell lines, RTgill-W1 and RTL-W1. Chemosphere 155, 308–318.
Zhang, J., et al., 2018. Occurrence of benzothiazole and its derivates in tire wear, road dust, and roadside soil. Chemosphere 201, 310–317.